

MODELING COMBUSTION CHAMBER DYNAMICS OF IMPINGING STREAM VORTEX ENGINES FUELED WITH HYDRAZINE-ALTERNATIVE HYPERGOLS

C.-C. Chen, M. J. Nusca, and M. J. McQuaid
US Army Research Laboratory
Aberdeen Proving Ground, MD 21005

ABSTRACT

To advance the development of Impinging Stream Vortex Engines (ISVEs) for tactical missile propulsion system applications, a computational fluid dynamics (CFD) modeling capability has been developed and employed to simulate the combustion chamber dynamics of various ISVE designs. Simulations of first-generation ISVE configurations fueled with monomethylhydrazine/red fuming nitric acid (MMH/RFNA) led to insights that inspired a combustion chamber design change, and simulations of an ISVE with the new feature validate its benefits. The CFD model has also been adapted to simulate the dynamics of ISVEs which incorporate a valving concept that is being developed to facilitate start-up and throttling. Additionally, because the risk to Soldier health posed by MMH is now considered unacceptable, the fuel upon which ISVE development program is currently predicated is a TMEDA-DMAZ blend. Toward modeling ISVEs fueled with this blend, a full, detailed chemical kinetics mechanism for TMEDA-DMAZ/RFNA systems was developed based on computational chemistry techniques and validated by reference to experimental data.

1. INTRODUCTION

Led by the U.S. Army Aviation and Missile Research, Development, and Engineering Center (AMRDEC), the Army is developing a novel hypergolic propulsion system concept for use in tactical missile systems (Michaels and Wilson, 1995; Nusca and McQuaid, 2007). Being fueled with a pumpable (re: liquid or gelled) fuel and a pumpable oxidizer that ignite spontaneously when mixed at ambient temperatures and pressures, hypergolic propulsion systems can be reliably shut down and restarted and/or throttled in flight. As such, they have the potential to offer more targeting options and range than the solid propellant-based rocket motors currently employed to propel tactical missiles. Because the fuel and oxidizer in hypergolic propulsion systems are stored in separate tanks, such systems are also inherently insensitive to a variety of stimuli that can produce catastrophic events

in solid-propellant-fueled rocket motors. The space required for traditional hypergolic propulsion system designs, however, prevents them from being integrated into airframes as small as those of tactical missiles. AMRDEC's concept, which is referred to as the Impinging Stream Vortex Engine (ISVE), appears capable of changing this paradigm.

The primary difference between the ISVE concept and conventional impinging stream engines (ISEs), both of which have fuel and oxidizer injection ports located in the radial wall of their combustion chamber, is the orientation at which the fuel and oxidizer are injected. In ISEs the injectors point towards the chamber's axial centerline while in the ISVE they are oriented tangential to the (radial) chamber wall. The ISVE configuration forces the propellants to mix in a highly turbulent vortex between the injector orifices and the chamber wall, and there has been some experimental evidence that centrifugal forces act to separate the heavier solid particles from the gas and move them toward the chamber wall. These flow properties have two benefits. First, they promote an increase in the mixing path length, which enables better performance to be obtained from the same-sized combustion chamber. Second, the unreacted propellant flow in an ISVE acts to cool the chamber walls, enabling them to be designed with thinner, lighter components than those needed for a conventional design.

Since the benefits of the ISVE concept accrue from characteristics of the propellant flow fields that it generates, a detailed understanding of the relationships between design parameters (such as the combustion chamber's dimensions and the angle of the injectors with respect to each other and the chamber walls) and the flow fields which result was considered needed in order to optimize the concept for specific applications. Such knowledge being difficult (if not impossible) to gain from nominally instrumented motor firings, the U.S. Army Research Laboratory (ARL) developed a CFD modeling capability as a means to elucidate such relationships. Derived from ARL-NSRG3, which is a time-accurate CFD code that has been adapted to

simulate unsteady, multi-component, chemically reacting flows in various gas-dynamic applications, the capability has previously been applied to simulate the combustion chamber dynamics of first-generation ISVE designs fueled with monomethylhydrazine/red fuming nitric acid (MMH/RFNA). (RFNA is composed primarily of nitric acid [HNO₃] and nitrogen dioxide [NO₂].) Results representing key findings of studies involving an ISVE (referred to as No. 1) are shown in Figures 1 and 2. As discussed in detail elsewhere (Nusca and Michaels, 2004), Figure 1 shows that when coupled to a single-step chemical kinetics mechanism with an empirically adjusted rate constant, the CFD model can reproduce the steady-state pressure but not the pressure transient observed during the ignition phase of the process. However, when coupled to a detailed, (multi-step) chemical kinetics mechanism, the model well-reproduces the measured chamber pressure throughout the ballistic cycle, and it does so without recourse to empirically adjusted parameters. Per results such as those of Figure 2, it was recognized that relatively high pressures are produced at the interface between the radial wall and the flat head (end) of ISVE No. 1's combustion chamber. (This location also happens to be where the pressure was measured in the test.)

Based on observations from test firings and CFD simulations of first-generation configurations, AMRDEC has incorporated several new features into its latest ISVE designs. One is a valving system that can vary the number of injector pairs that feed the combustion chamber during the course of a ballistic cycle. Referred to as the Sliding Actuator Multi-Mode Injection Throttling Technique (SLAMMITT) (Mathis et al., 2007; Mathis et al. 2008), the concept was proposed as a means to avoid hard starts and to enable incremental thrust level variations. In addition, the combustion chamber of one of the ISVEs built to test and develop the SLAMMITT concept was designed with a domed head, the thought being that such a configuration would reduce flow stagnation at the interface between the radial wall and the head, and thereby reduce the pressure gradients and perhaps the pressure spiking observed in flat-head configurations.

The bipropellant combination with which new ISVEs are being fueled is another change that has been instituted in the development program. Although MMH/RFNA works well and its performance is not expected to be exceeded by other candidates, because of MMH's carcinogenic potential, the risk it poses to Soldier health has come to be deemed unacceptable. Therefore, alternatives to it are being sought. The two classes of compounds considered to have the best prospects for meeting desired performance objectives

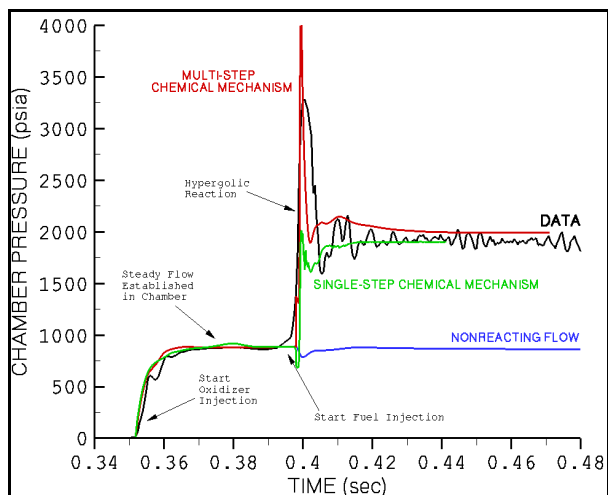


Figure 1. Measured and simulated pressure traces for an ISVE No. 1 test firing.

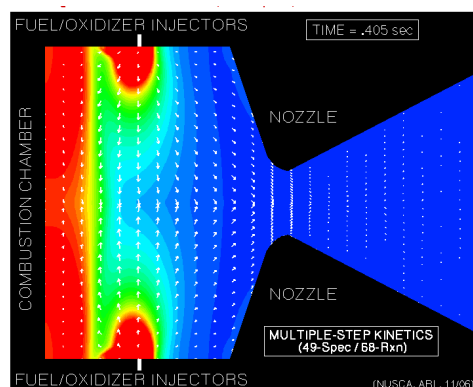


Figure 2. Pressure contours in ISVE No. 1 during steady-state operation. (Blue to red: 0 to 2 kpsia)

while having risks to human health and the environment that are acceptable are saturated, aliphatic or aliheterocyclic amines (SAs) and ethanamine azides (EAs) (McQuaid, 2006). The candidate in which AMRDEC has the most confidence at this time is a SA-EA blend, the SA being N₁N₂N₁'N₂'-tetramethyl-1,2-ethylenediamine (TMEDA) and the EA being 2-azido-N,N-dimethylethanamine (DMAZ). The chemical structures of these two compounds are shown in Figure 3.

Toward providing continued CFD modeling support for the ISVE development program, ARL has incorporated into its CFD model the capability for simulating the new design features AMRDEC is testing. In the sections which follow, the implementation and validation of additions to the model are discussed, and simulation results that have influenced the course of AMRDEC's development program are presented.

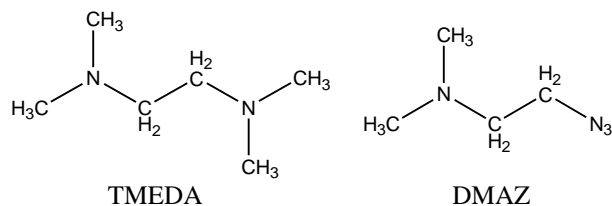


Figure 3. The chemical structures of TMEDA and DMAZ.

2. DOMED-HEAD CONFIGURATION AND SLAMMITT

AMRDEC built two different ISVE designs to test the SLAMMITT concept: one with a flat head and the other with a domed head. The domed-head design is depicted schematically in Figure 4. The head is a 2:1 ellipse, the chamber is 5-cm in diameter, and the combustion chamber/nozzle combination is about 14-cm long. The length of the combustion chamber/nozzle of its flat-head counterpart is about 13 cm long. As such, the volumes of these designs are about seven times larger than those of ISVE No. 1 (Nusca et al., 2007). The grid employed to model the domed-head design had 180 azimuthal planes, with each having 203 cells along the chamber axis and 200 cells across the chamber diameter, for a total of about 7 million grid cells.

As a first step toward examining how the combustion chamber dynamics in the two new designs

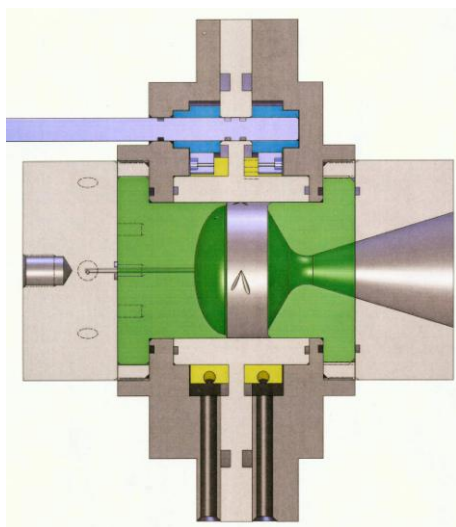


Figure 4. Schematic depiction of ISVE domed head design.

compare with those observed in ISVE No. 1, the internal flow-fields of the two when fueled with MMH/RFNA were simulated. Figure 5 compares the pressure history computed at a point of the interface between the head and radial wall when the injection schedule for the new designs is analogous to the one employed in generating the results for Figure 1. In the case of the larger flat head design, the pressure observed prior to the injection of MMH is similar to that observed in ISVE No. 1. Subsequent to the fuel's injection, however, the pressure transient associated with ignition is larger, and the steady-state pressure is higher. In the domed-head design, a steady-state pressure similar to the one produced in ISVE No. 1 is achieved, but the pressure observed prior to the injection of MMH is much lower than it is the two flat head designs because the oxidizer does not have a "corner" to accumulate in. Moreover, there is no pressure spike produced during the ignition phase.

Figure 6 shows representative CFD results for the flow-field within the domed-head ISVE at about 0.45 seconds after the oxidizer's injection onset. (At this time, flow field conditions are relatively steady.) Pressures are observed to be relatively high near the injectors and in the flow stagnation region near the head end of the chamber. But the head end pressures are much lower than those observed in ISVE No. 1. In addition, the computed contours of the combustion product OH indicate that the head end of the engine is a well-stirred vortical region. Taken together, the results validate the effectiveness of the domed-head in

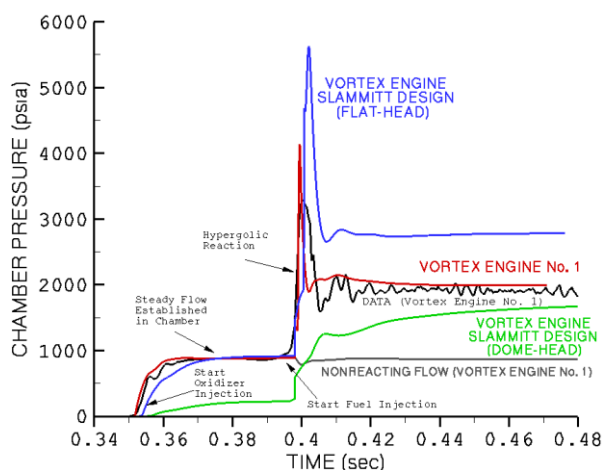


Figure 5. Comparison of simulated chamber pressures for flat-head and domed-head designs with measured values for ISVE No. 1.

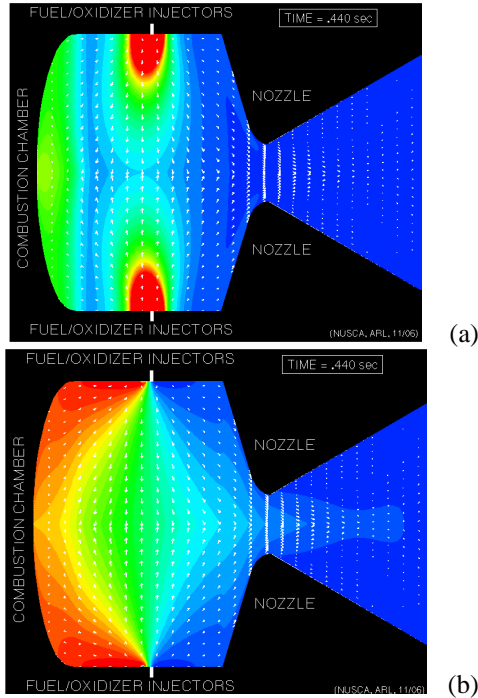


Figure 6. Contours and selected velocity vectors during steady-state operation for a domed-head ISVE: (a) Pressure (Blue to red: 0 to 2 kpsia); (b) OH fraction (Blue to red: 0 to 0.25).

mitigating the flow stagnation that leads to high local pressure in the two flat-head designs, and they were a basis for AMRDEC’s decision to conduct all future testing of the SLAMMITT concept with the domed-head design.

Next, the dynamics of the SLAMMITT-equipped domed-head design was simulated with propellant injection schedules that were actually employed in test firings. Figure 7(a) shows results from a simulation of an MMH/RFNA-fueled test in which two different thrust levels were produced by varying the number of operational injectors. The simulation’s pressure histories well-reproduce the histories that were measured. (The measured pressure and thrust data, which may be found in (Mathis et al., 2007) and (Mathis et al. 2008), are not reproduced in this paper.) Measured thrust levels were about 100 lb_f during the two “low-thrust” intervals and about 400 lb_f during the “high-thrust” interval. The computed thrust levels—see Figure 7(a), “Thrust Method 1”—are slightly higher than the values measured, with the largest discrepancies occurring in the simulation of the second low-thrust interval. The “top hat” shape in the thrust curve demonstrates that the engine responds rapidly to the change in the number of operational injectors.

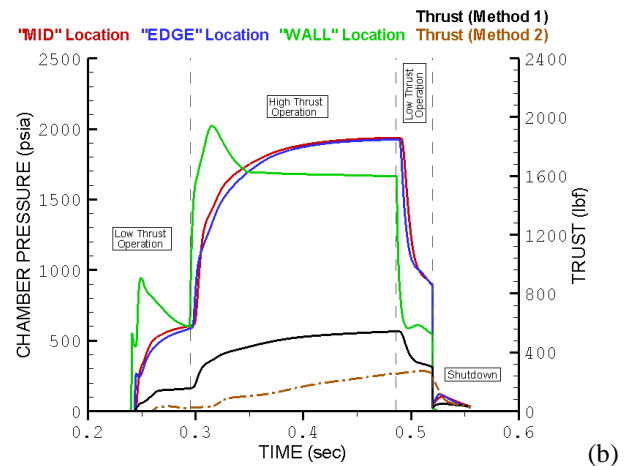
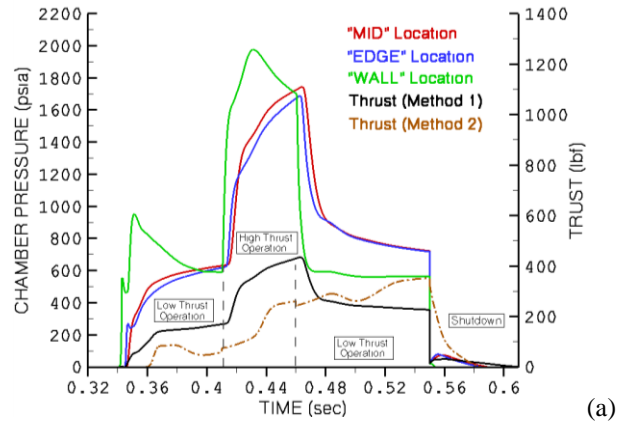


Figure 7. Simulated chamber pressures and thrust levels for the domed-head SLAMMITT ISVE design fueled with MMH/RFNA: (a) short throttling intervals employed in an MMH/RFNA-fueled test, (b) extended high-thrust interval employed in a TMEDA-DMAZ/RFNA-fueled test.

The simulation of another test firing is shown in Figure 7(b). In this test (Mathis et al., 2008), the ISVE was fueled with TMEDA-DMAZ/RFNA instead of MMH/RFNA and the throttling schedule included an extended high-thrust interval. Because a TMEDA-DMAZ/RFNA chemical kinetics mechanism was not available for the CFD model at the time this work was performed, the MMH/RFNA mechanism was employed for the simulation. Nevertheless, the simulated thrust levels were found to be only 2% to 5% higher than the values measured in the test. Considered plausible because the performance characteristics of TMEDA-DMAZ/RFNA and MMH/RFNA are (on the basis of equilibrium computations) theoretically quite similar, details of the flow field revealed by the simulation are being taken into account by AMRDEC as it attempts to advance the SLAMMITT concept.

3.0 TMEDA-DMAZ/RFNA CHEMICAL KINETICS MECHANISM

To develop a chemical kinetics mechanism for TMEDA-DMAZ/RFNA, separate TMEDA/RFNA and DMAZ/RFNA mechanisms were developed first and then combined. The basic approach to developing the TMEDA/RFNA and DMAZ/RFNA mechanisms followed from insights ARL gained from developing a mechanism for MMH/RFNA (Ishikawa and McQuaid, 2006; and references therein). Among them are that various exothermic complexation reactions and addition reactions provide the energy needed to promulgate H-atom abstraction from the fuel (parent) and its dehydrogenated daughters. The daughters further decompose via β -scission reactions, and radicals from those reactions are oxidized to complete the combustion process.

The challenges to developing mechanisms for TMEDA/RFNA and DMAZ/RFNA were, however, much bigger than those posed by MMH/RFNA. MMH's preeminence as a hypergol had led to many previous studies of its combustion chemistry, and a large part of the mechanism could be constructed from them. ARL needed only to supplement the published information, refining parameters for certain reaction steps and adding a small set of reactions so that simulations more closely approximated the behavior of experimentally characterized systems. Very little has been reported on the combustion of amines (in general) let alone TMEDA or DMAZ oxidized by RFNA. Therefore, the mechanisms for them had to be built essentially from scratch. An additional difficulty was that TMEDA and DMAZ are much larger molecules than MMH: both of them having eight heavy (non-hydrogen) atoms vs. the three in MMH. Thus there are many more potential pathways for their decomposition to take.

Because of the extent and complexity of the studies performed to build and validate the TMEDA/RFNA and DMAZ/RFNA mechanisms, the focus here is on the postulation of a couple of small subsets of reactions that were expected to be important, but for which rate constants had not been previously established. Common to all such work was the use of computational chemistry to characterize reaction intermediates and paths for their decomposition. Molecular structures and normal mode frequencies for intermediates considered likely to be important in a reaction system were calculated via density functional theory methods including B3LYP/6-31G(d,p) and MPWB1K/6-31+G(d,p). Refined energy characterizations were then obtained with B3LYP/6-311+G(2df,p), G3, G3MP2

and CBS-Q models. CCSD(T) calculations with relatively large basis sets were also performed for (small) molecules for which they were practical. All results reported here were obtained via calculations performed with the Gaussian 03 suite of quantum chemistry (QC) codes (Frisch et al., 2003).

Once molecular structures of relevant species were characterized, their entropies and heat capacities were calculated from methods of macro-canonical statistical mechanics using vibration frequencies, moments of inertia, and internal rotation parameter data obtained from the QC calculations and the open literature when available. The thermochemical data were then utilized in conjunction with: (1) the principles of thermochemical kinetics, (2) transition state theory (TST), and (3) quantum Rice-Ramsberger-Kassel (QRRK) unimolecular rate theory with master equation analysis to calculate kinetic parameters for postulated reactions. Unimolecular dissociation and isomerization reactions of chemically activated and stabilized adducts that result from addition or recombination reactions were analyzed by first constructing potential energy diagrams for them. Kinetics parameters for unimolecular and bimolecular (chemical activation) reactions were then calculated via multi-frequency QRRK analysis for $k(E)$ (Westmoreland et al., 1986; Westmoreland, 1992; Dean and Westmoreland, 1987). The master equation analysis discussed by Gilbert was used for fall-off (Gilbert and Smith, 1990; Chang et al., 2000; Gilbert et al., 1983).

3.1 TMEDA/RFNA

Based on the work to develop the MMH/RFNA mechanism, reactions between NO_2 and the first daughters of H-atom abstraction from the fuel (TMEDA): i.e., $(\text{CH}_3)_2\dot{\text{N}}\text{CHCH}_2\text{N}(\text{CH}_3)_2$ and $\text{H}_3\text{CN}(\dot{\text{C}}\text{H}_2)\text{CH}_2\text{CH}_2\text{N}(\text{CH}_3)_3$, were expected to be important for TMEDA/RFNA systems. The potential energy diagram that was determined for $(\text{CH}_3)_2\dot{\text{N}}\text{CHCH}_2\text{N}(\text{CH}_3)_2 + \text{NO}_2$ reactions is shown in Figure 8. As indicated, the first step involves NO_2 attaching to $(\text{CH}_3)_2\dot{\text{N}}\text{CHCH}_2\text{N}(\text{CH}_3)_2$'s radical site and forming $(\text{CH}_3)_2\text{NCH}(\text{ONO})\text{CH}_2\text{N}(\text{CH}_3)_2^*$ or $(\text{CH}_3)_2\text{NCH}(\text{NO}_2)\text{CH}_2\text{N}(\text{CH}_3)_2^*$. The well-depths for these adducts are ~ 57 kcal/mol at 298 K, with the $(\text{CH}_3)_2\text{NCH}(\text{ONO})\text{CH}_2\text{N}(\text{CH}_3)_2^*$ adduct being lower in energy by ~ 0.6 kcal/mol.

As shown in Figure 8, $(\text{CH}_3)_2\text{NCH}(\text{NO}_2)\text{CH}_2\text{N}(\text{CH}_3)_2^*$ can subsequently (1) dissociate back to reactants, (2) stabilize to $(\text{CH}_3)_2\text{NCH}(\text{NO}_2)\text{CH}_2\text{N}(\text{CH}_3)_2$, or (3) eliminate *trans*-HONO to produce $(\text{CH}_3)_2\text{NCH}=\text{CHN}(\text{CH}_3)_2$. Based on G3MP2//B3DP

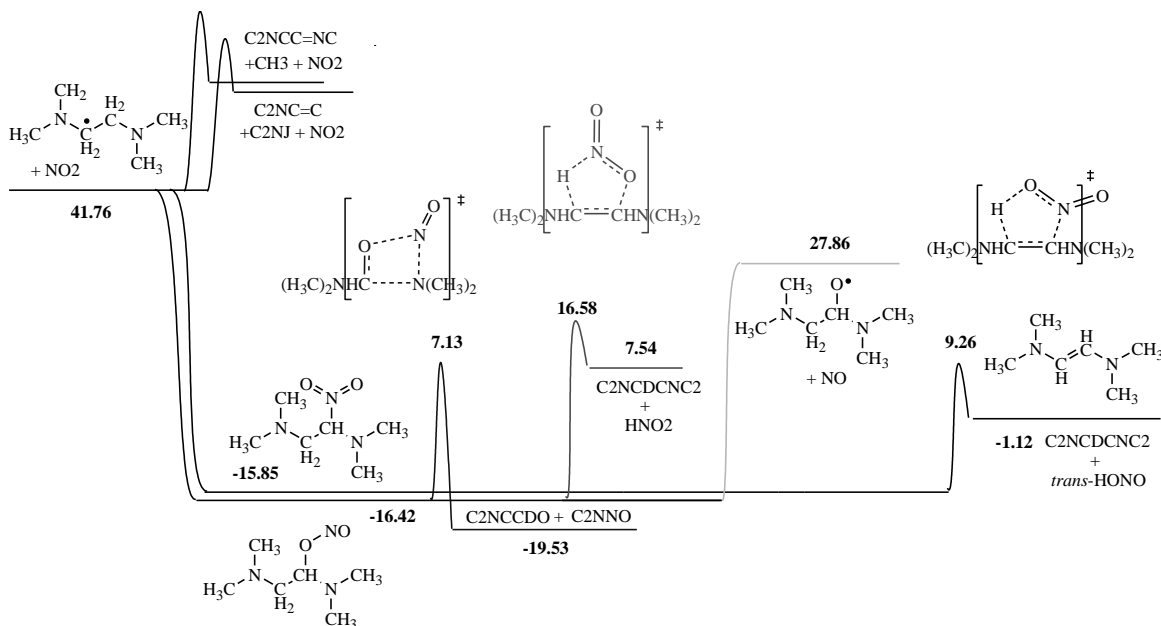


Figure 8. Potential energy diagrams for the $(\text{CH}_3)_2\text{NCHCH}_2\text{N}(\text{CH}_3)_2 + \text{NO}_2$ system. (Energy units are kcal/mol.)

calculations, the barrier to this reaction is 26 kcal/mol, and overall it is 15 kcal/mol endothermic. The $(\text{CH}_3)_2\text{NCH}(\text{ONO})\text{CH}_2\text{N}(\text{CH}_3)_2^*$ adduct can: (1) dissociate back to reactants, (2) stabilize to $(\text{CH}_3)_2\text{NCH}(\text{ONO})\text{CH}_2\text{N}(\text{CH}_3)_2$, (3) proceed via a four-member ring transition state to $(\text{CH}_3)_2\text{NN}=\text{O} + (\text{CH}_3)_2\text{NCH}_2\text{CH}=\text{O}$, (4) eliminate HNO_2 via a five-member ring to produce $(\text{CH}_3)_2\text{NCH}=\text{CHN}(\text{CH}_3)$, or (5) dissociate to $(\text{CH}_3)_2\text{NCH}(\text{O}\cdot)\text{CH}_2\text{N}(\text{CH}_3)_2$ and NO .

From such results, rate constants for all postulated reactions were determined, and with the addition of many small molecule reactions assembled in the development of the MMH/RFNA mechanism, a chemical kinetics mechanism for TMEDA/RFNA was constructed. Comprised of ~1400 reactions and involving over 400 species, evidence for the mechanism's validity was sought by employing it with CHEMKIN to predict time-to-ignition values for various initial conditions and comparing those values to results observed in drop-into-drop ignition delay tests. Figure 9 shows some relevant results from a simulation of a 20-wt% TMEDA/67-wt% HNO_3 /11-wt% N_2O_4 /2-wt% H_2O mixture initially at 300 K and 75 atm. The simulation predicts that the system's time-to-ignition will be a little over 30 ms. This duration is longer than that observed for comparable MMH/RFNA systems, which is to be expected, and its magnitude is in line with expectations based on ignition delays that have been measured in TMEDA/RFNA drop-into-drop tests. As such, the mechanism was considered a reasonable

basis upon which to derive a reduced mechanism for simulating the kinetics occurring in TMEDA/RFNA-fueled ISVEs.

3.2 DMAZ/RFNA

Because various details of the unimolecular paths by which an azide may decompose have been a matter of some debate, this aspect of the development of the DMAZ/RFNA mechanism was of particular interest and concern. Paths that were identified and characterized included: (1) simple scissions of C-H, C-N or C-C bonds, (2) N-N bond fissions via either a concerted

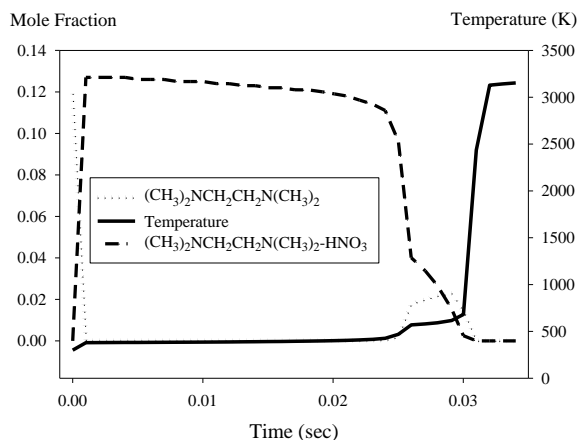


Figure 9. CHEMKIN simulation of a TMEDA/RFNA system.

(synchronous) reaction [DMAZ \rightarrow singlet imine ($R_2C=NH$) + N_2] or a stepwise (asynchronous) reaction [DMAZ \rightarrow nitrene intermediate ($R-N:$) + N_2], (3) HN_3 molecular elimination with the formation of dimethylaminoethylene, and (4) N_2 elimination with cyclization to form molecules with three- or four-member heterocyclic rings. A QRRK analysis showed that N_2 elimination concurrent with a 1,2 H-shift is dominant at temperatures below 2000 K. The stepwise path with nitrene ($R-N:$) formation becomes dominant at temperatures above 2000K, but the nitrene converts to the imine. Therefore, the shift in the relative importance of the two steps does not lead to a shift to an alternate secondary chemistry.

To corroborate the validity of the rate constants for the decomposition steps, the DMAZ/RFNA mechanism was employed with CHEMKIN to simulate results reported for the decomposition of DMAZ in a flow reactor (Striebich and Lawrence, 2003). (Though DMAZ was solvated in dodecane in the experiment, we assume that dodecane does not exert a catalytic influence on the decomposition.) As shown in Figure 10, simulations based on the theoretical results well-reproduce the experimental data.

3.3 TMEDA-DMAZ/RFNA

A full, multi-step, chemical kinetics reaction mechanism for TMEDA-DMAZ/RFNA was constructed by combining the TMEDA/RFNA and DMAZ/RFNA mechanisms. The result is comprised of nearly 2000 reaction steps and involves over 450 species. When employed with CHEMKIN to simulate the behavior of TMEDA-DMAZ/RFNA systems, the mechanism predicts time-to-ignition values that are shorter than those for comparable TMEDA/RFNA and DMAZ/RFNA

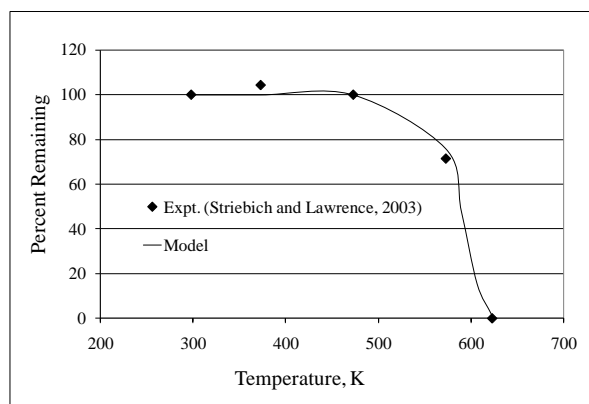


Figure 10. Percent decomposition of DMAZ for a given reactor input mass flow rate.

systems. Such results are consistent with observations from drop-into-drop ignition delay experiments. So validated, the reduction of the mechanism for use in the CFD model has been initiated.

SUMMARY

CFD simulations of chemically reacting flows within the combustion chambers of the latest generation of ISVEs have yielded insights into the benefits of a new chamber-head design and the SLAMITT concept. The simulations demonstrate that the domed-head design is effective in mitigating the stagnated flow that leads to high local pressure in ISVE's having flat heads. Simulations that indicate the responsiveness of the combustion chamber dynamics to changes in the number of operational injectors enabled via SLAMITT are also instructive. In addition, a full, multi-step, TMEDA-DMAZ/RFNA chemical kinetics mechanism was developed and validated. Comprised of nearly 2000 reaction steps and involving over 450 species, it is being reduced to enable the modeling of ISVEs fueled with this alternative to MMH/RFNA.

ACKNOWLEDGEMENTS

Dr. W. Anderson (ARL) formulated the initial full MMH/RFNA chemical kinetics mechanism from which Dr. A. Kotlar (ARL) derived the reduced MMH/RFNA chemical reaction mechanism used with the CFD code. Mr. R. S. Michaels, Mr. N. Mathis and Ms. L. Felton (AMRDEC) provided helpful information concerning the ISVE and its propellants. The effort was partially funded under an Environmental Quality Technology program managed by Ms. M. Miller (RDECOM). Dr. Chen was supported through the Postgraduate Research Participation Program administered by the Oak Ridge Institute for Science and Education. The DoD HPC Modernization Office also supported this effort by supplying supercomputer time under the Computing Challenge Project C2N. The computer time was made available at the DoD Major Shared Resource Center at the Air Force Research Laboratory, Wright-Patterson Air Force Base, OH and the Distributed Center at the AHPCRC.

REFERENCES

- Chang, A. Y., Bozzelli, J. W., and Dean, A. M., 2000: Kinetic Analysis of Complex Chemical Activation and Unimolecular Dissociation Reactions Using QRRK Theory and the Modified Strong Collision Approximation, *Z. Physik. Chem.*, **214**, 1533-1568.

- Dean, A. M., and Westmoreland, P. R., 1987: Bimolecular QRRK Analysis of Methyl Radical Reactions, *Int. J. Chem. Kinet.*, **19**, 207.
- Frisch, M. J., et al., 2003: Gaussian 03, Revision B.05, Gaussian, Inc., Pittsburgh PA.
- Gilbert, R. G., and Smith, S. C., 1990: *Theory of Unimolecular and Recombination Reactions*, Oxford Press.
- Gilbert, R. G., Luther, K., and Troe, J., 1983: Theory of Thermal Unimolecular Reactions in the Fall-off Range. 2. Weak Collision Rate Constants, *Ber. Buns-Phys. Chem. Chem. Phys.* **87**, 1669-177.
- Ishikawa, Y. and McQuaid, M. J., 2006: H-Atom Abstraction from CH₃NHNH₂ by NO₂: CCSD(T)/6-311++G(3df,2p)//MPWB1K/6-31+G(d,p) and CCSD(T)/6-311+G(2df,p)//CCSD/6-31+G(d,p) Calculations, *J. Phys. Chem. A*, **110**, 6129-6138.
- Mathis, N. P., Turner, T. W., Michaels, R. S., and Arszman, J.H., 2007: Development and Demonstration of Vortex Engine Throttling Techniques,” *Proceedings of the 3rd JANNAF Liquid Propulsion Subcommittee Meeting*, CPIA Publication JSC CD-49.
- Mathis, N. P., Turner, T. W., Michaels, R. S., and Arzman, J.H., 2008: Throttling and Ignition Delay Mitigation in SLAMMITT Vortex Engines,” *Proceedings of the 55th JANNAF Propulsion Meeting*, CPIA Publication (in press).
- McQuaid, M. J., 2006: Notional Hydrazine-Alternative Hypergols: Design Considerations, Computationally-Based Property Determinations, and Acquisition Possibilities, ARL-TR-3694, Aberdeen Proving Ground, MD.
- Michaels, R. S. and Wilson, B. F., 1995: The Low L/D Vortex Engine for Gel Propulsion, *Proceedings of the 1995 JANNAF Gel Propulsion Technology Symposium*, CPIA Pub. 627, pp. 9-16.
- Nusca, M. J. and Michaels, R. S., 2004: Development of a Computational Model for the Army’s Impinging Stream Vortex Engine,” *Proceedings of the 1st JANNAF Liquid Propellant Subcommittee Meeting*, CPIA Publication JSC CD-33
- Nusca, M. J., and McQuaid, M. J., 2007: Combustion Chamber Fluid Dynamics and Hypergolic Gel Propellant Chemistry Simulations for Selectable Thrust Rocket Engines, *Proceedings of the HPCMP Users Groups Conference*, IEEE Computer Society, Pittsburgh, PA.
- Nusca, M. J., Mathis, N. P., and Michaels, R. S., 2007: Computational Modeling of the Army’s Impinging Stream Vortex Engine Including an Injection Throttling System, *Proceedings of the 3rd JANNAF Liquid Propulsion Subcommittee Meeting*, CPIA Publication JSC CD-49.
- Striebich, R. C. and Lawrence, J., 2003: Thermal Decomposition of High-energy Density Materials at High Pressure and Temperature, *J. Anal. Appl. Pyrolysis* **70**, 339-352.
- Westmoreland, P. R., Howard, J. B., Longwell, J. P., and Dean, A.M., 1986: Prediction of Rate Constants for Combustion and Pyrolysis Reactions by Bimolecular QRRK, *AICHE Journal*, **32**, 1971-1979.
- Westmoreland, P. R., 1992: Thermochemistry and Kinetics of C₂H₃+O₂ Reactions, *Combust. Sci. and Tech.* **82**, 151-168.